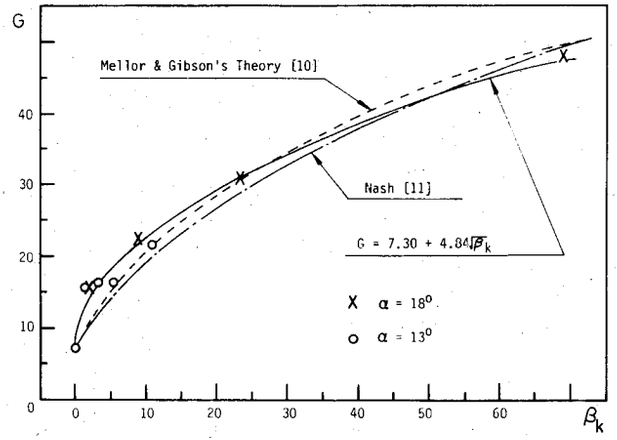

Fig. 3 Correlation of defect shape factor with pressure gradient parameter.

The defect shape factor G defined in Eq. (2) is generally used to show the effects of pressure gradient,

$$G=\int_0^{\delta}\left(\frac{U_e^*-\bar{U}^*}{U_\tau}\right)^2 \mathrm{d}\left(\frac{y}{\Delta}\right) \qquad (2)$$

where the defect thickness Δ is defined as

$$\int_0^{\delta}(U_e^*-\bar{U}^*)/U_\tau \mathrm{d}y$$

The values of G are plotted in Fig. 3 against the compressible pressure gradient β_k, as suggested by Alber and Coats.[5]

Results and Discussions

In the above analysis, one may have reservations about the values of wall shear stress obtained with the assumption of a constant pressure boundary layer. But, considering the inevitable complexity of flowfield, the results as seen in Fig. 2 are encouraging in comparison with some direct measurements with a Preston tube[6] or with a heated-wire gage[7] in milder pressure gradient than this case:

1) The profiles of $\alpha=13$ deg (in Fig. 2) show a large increase in wake components as found in incompressible flows with an adverse pressure gradient. But the sublayer grows in relative thickness in contrast to the subsonic case. This fact was also noted in Ref. 2. When there exists a separation bubble ($\alpha=18$ deg), the profiles are mostly concave and have lower values than the law of the wall. So it could be said that the sublayer becomes thicker and covers a large part of the boundary layer downstream of the separation bubble.

2) Correlation of defect shape factor G with pressure gradient parameter β_k is obtained in the form of $G=7.30+4.84\sqrt{\beta_k}$ for $0<\beta_k<70$, as can be seen in Fig. 3. The maximum β_k is about 70, and such high values of β_k could not be found in similar analysis of compressible turbulent boundary layer. For example, the maximum β_k was 3.5 in Ref. 8, about 2 in Ref. 4, and 1.8 in Ref. 9. So the values of G are compared with the theory and experimental results of incompressible flow. The correlation obtained from the analysis shows good agreement with Mellor and Gibson's theory[10] for equilibrium incompressible flow and also with Nash's correlation[11] for incompressible flows.

References

[1] Ardonceau, P., Lee, D. H., de Roquefort, T. A., and Goethals, R., "Turbulence Behavior in a Shock-Wave/Boundary Layer Interaction," *Turbulent Boundary Layers—Experiments, Theory, and Modelling*, AGARD CP 271, 1979.

[2] Fernholz, H. H. and Finley, P. J., "A Critical Commentary on Mean Flow Data for Two-Dimensional Compressible Turbulent Boundary Layers," AGARDograph No. 253, 1980.

[3] Maise, G. and McDonald, H., "Mixing Length and Kinematic Eddy Viscosity in a Compressible Boundary Layer," *AIAA Journal*, Vol. 6, Jan. 1968, pp. 73-79.

[4] Lewis, J. E., Gran, R. L., and Kubota, T., "An Experiment on the Adiabatic Compressible Turbulent Boundary Layer in Adverse and Favourable Pressure Gradients," *Journal of Fluid Mechanics*, Vol. 51, Pt. 4, 1972, pp. 657-672.

[5] Alber, I. E. and Coats, D. E., "Analytical Investigation of Equilibrium Compressible Turbulent Boundary Layers," AIAA Paper 69-689, 1969.

[6] Peake, D. J., Brakmann, G., and Romeskie, J. M., "Comparisons between Some High Reynolds Number Turbulent Boundary Layer Experiments at Mach 4 and Various Recent Calculation Procedures," National Research Council of Canada and AGARD CP-93-71, 1971, Paper 11.

[7] Kussoy, M. I., Horstman, C. C., and Acharya, M., "An Experimental Documentation of Pressure Gradient and Reynolds Number Effects on Compressible Turbulent Boundary Layer," NASA TM 78488, 1978.

[8] Struek, W. B. and Danberg, J. E., "Supersonic Turbulent Boundary Layer in Adverse Pressure Gradient, Pt. II: Data Analysis," *AIAA Journal*, Vol. 10, May 1972, pp. 630-635.

[9] Laderman, A. J., "Adverse Pressure Gradient Effects on Supersonic Boundary Layer Turbulence," *AIAA Journal*, Vol. 18, Oct. 1980, pp. 1186-1195.

[10] Mellor, G. L. and Gibson, D. M., "Equilibrium Turbulent Boundary Layers," *Journal of Fluid Mechanics*, Vol. 24, Pt. 2, 1966, pp. 225-253.

[11] Nash, J. F., "Turbulent-Boundary-Layer Behavior and the Auxiliary Equation," AGARDograph 97, 1965, pp. 245-279.

Global Distribution of Stratospheric Aerosols by Satellite Measurements

M. P. McCormick*
NASA Langley Research Center, Hampton, Virginia

Introduction

In the lower to middle stratosphere there exists a region of increased concentration of large particles greater than about 0.1-μm radius. This layer of large particles is called the stratospheric aerosol layer or Junge layer.[1] Therein, the mixing ratio reaches a peak at approximately 10 km above the local tropopause of about 6-10 particles/mg of air during nonvolcanic periods which corresponds to peak concentrations of about 0.5 particles/cm^3 (Ref. 2). The size distributions for these particles generally are described by an analytical function chosen to fit a set of experimental data. A lognormal distribution seems to fit a large number of observations and agrees with many other size distribution functions for radii between 0.1 and 0.6 μm. This size region is the dominant contributor to stratospheric aerosol extinction and backscatter at red and near-infrared wavelengths.[3] The exact composition of the aerosol particles is not known but most evidence supports an aerosol composed of a 75% sulfuric acid and 25% water solution.[4] The primary source of sulfur that establishes the background layer is thought to be tropospheric OCS (carbonyl sulfide), but it is becoming less clear as to whether or not volcanoes are the primary source. In either case, gas phase H_2SO_4 is formed which then par-

Presented as Paper 82-0086 at the AIAA 20th Aerospace Sciences Meeting, Orlando, Fla., Jan. 11-14, 1982; submitted Jan. 22, 1982; revision received July 16, 1982. This paper is declared a work of the U.S. Government and therefore is in the public domain.

*Head, Aerosol Research Branch, Atmospheric Sciences Division.

ticipates in the microphysical processes of nucleation and condensation which lead to particle formation and growth.

Volcanic eruptions can enhance the stratospheric aerosol layer by orders of magnitude by injecting SO_2 and/or H_2SO_4 directly into the stratosphere. Global stratospheric optical depths easily can change from 1-μm wavelength background values of 0.0013 to greater than 0.1 after an eruption.[5] The potential for these particles to cause significant temperature changes in the stratosphere or troposphere, however, depends on their stratospheric residence time and optical properties and the albedo of the underlying surface/atmosphere. To cause a significant change, there must be enough material present for periods in excess of the thermal response time of the atmosphere and/or surface. For the stratosphere, this is about a month, whereas for the troposphere it is about five years due to the thermal inertia of the oceans. Thus, the competing factors of lifetime and thermal response must be considered in determining whether a volcanic eruption will have any climatic impact.

This Note describes the first-ever global aerosol climatology that is being developed by two Earth-orbiting satellite sensors: stratospheric aerosol measurement II (SAM II) and stratospheric aerosol and gas experiment (SAGE). The data will show the normal background aerosol, its seasonal and hemispheric variations, the existence of polar stratospheric clouds (probably made up of ice particles), and the impact of volcanic eruptions (particularly the 1980 eruption of Mount St. Helens).

Experimental Description

The technique used by SAM II and SAGE is solar occultation, that is, a measurement of solar intensity is made during each spacecraft sunrise and sunset. SAM II and SAGE lock onto the sun in azimuth and scan vertically up and down across the sun as it sets or rises with a field-of-view of 0.5 arcmin which defines an instantaneous vertical resolution of 0.5 km. SAM II is a single spectral channel photometer with a passband centered at 1.0 μm, whereas SAGE has four spectral channels centered at 0.385, 0.45, 0.6, and 1.0 μm. SAM II is flying aboard the Nimbus 7 spacecraft which was launched Oct. 24, 1978, and is in a noon sun-synchronous orbit. For solar occultation measurements, the latitude coverage is constrained to the polar regions with sunsets occurring in the Arctic and sunrises in the Antarctic. SAGE is flying aboard the Applications Explorer Mission-2 satellite, launched Feb. 18, 1979, which is in a precessing 56 deg inclined orbit that provides measurement coverage between the polar regions. Thus, each spacecraft is providing approximately 15 sunrises and 15 sunsets (or measurement opportunities) each day that are spread over most of the globe in one month. A complete description of SAM II and SAGE is given in McCormick et al.[6]

The extinction coefficient at 1.0 μm, the primary aerosol channel for SAM II and SAGE, is made up of extinction from aerosols and Rayleigh scattering from molecules. The molecular contribution is determined from supporting meteorological atmospheric density data supplied by the National Oceanic and Atmospheric Administration. The aerosol extinction coefficient is the basic data product from the inversion of SAM II and SAGE data. It is related to the aerosol number density through modeling of aerosol size distribution and index of refraction assuming spherical particles. A complete description of the mathematical inversion of SAM II and SAGE data is given in Chu and McCormick.[7]

Global Observations

Figure 1 shows a typical inverted profile of aerosol extinction vs altitude from SAGE for May 1980 in the Northern Hemisphere. It represents background values during that period, free of the influence from the eruption of Mount St. Helens. It is not background in the truest sense of the word,

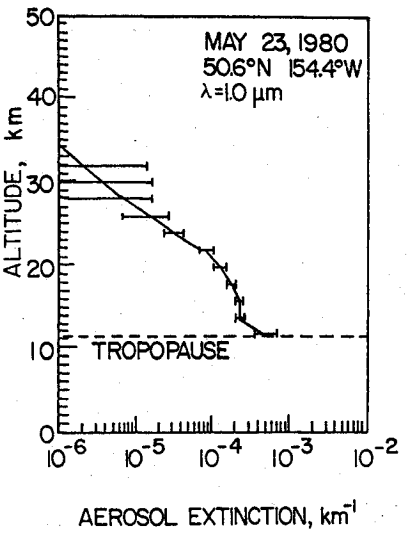

Fig. 1 Aerosol extinction for background conditions.

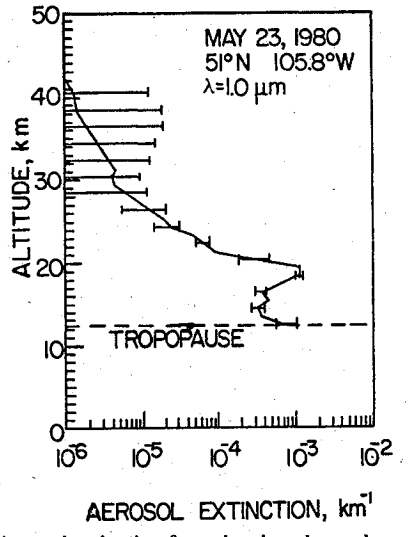

Fig. 2 Aerosol extinction for volcanic-enhanced conditions.

however, since there still exists a small influence from the November 1979 eruption of Sierra Negra on the Galapagos Islands. Note that the background extinction value is about 1-2×10^{-4} km^{-1} between 20 km and just above the tropopause. The horizontal bars associated with the extinction curve represent the $\pm 1\sigma$ limits of the inverted result. The "top" of the layer, defined as the altitude for which extinction drops by a factor of 10, is at about 27 km, about 15 km above the local tropopause. Figure 2 shows a similar plot for an earlier revolution of the spacecraft. On the same day, at 105.8-deg W longitude, the effects of the Mount St. Helens (MSH) eruption are easily seen. A large enhancement exists at 18-19 km with a value of about 10^{-3} km^{-1}, or 10 times the background values shown in Fig. 1. This is typical for the MSH's eruption. Material from the eruption below about 19 km moved eastward; the material in the 12-km altitude region circled the globe in about two weeks at an average speed of about 25 m/s. Some material penetrated to as high as 24 km and moved slowly westward at average speeds between 6 and 8 m/s. This material circled the globe in about 60-80 days. SAGE was able to detect the stratospheric material and subsequently monitor its global transport and dispersion. An example of a zonal average of extinction vs latitude and altitude is shown in Fig. 3 for the month of September 1980, 3.5-4.5 months after the May 18 eruption. The gas-to-particle, dispersion, and transport processes produced an aerosol

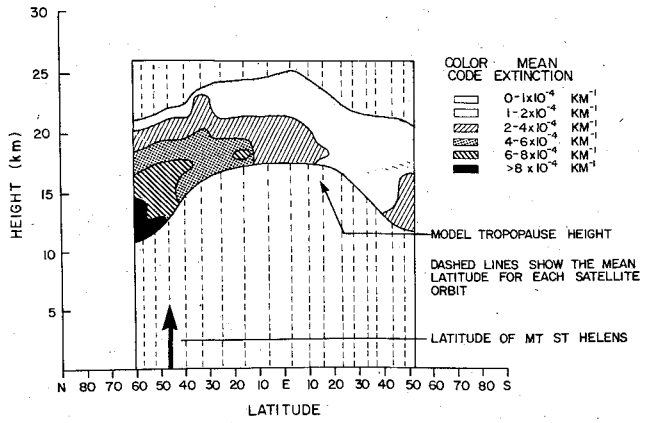

Fig. 3 Zonal averages of aerosol extinction for September 1980.

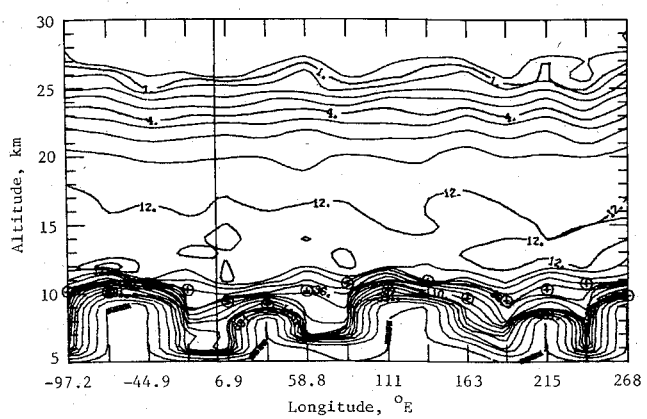

Fig. 4 Contours of aerosol extinction in the Arctic summer, Aug. 2-3, 1979.

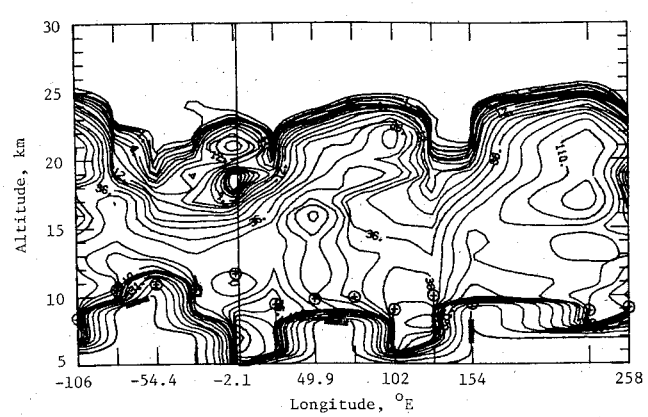

Fig. 5 Contours of aerosol extinction in the Antarctic winter, Aug. 1, 1979.

distribution that primarily was restricted to the Northern Hemisphere and heavily concentrated at the higher latitudes. Local enhancements of a factor greater than eight can be seen. This material amounted to a 100% mass increase in the Northern Hemisphere aerosol. The region of enhanced extinction at high latitudes in the Southern Hemisphere is due to stratospheric clouds and will be described later. Even though significant in mass, available one-dimensional radiative-convective models[8] predict that this amount of material would insignificantly affect the Earth's climate. This event, however, has provided a well-documented eruption that can be scaled to past, much larger eruptions. The conclusion is that these past eruptions could have caused significant climate effects. In addition to climate models, this eruption permits the use of SAGE data in the development of multi-dimensional transport models.

An example of the distribution of aerosols with longitude is shown in Fig. 4. Contours of aerosol extinction are plotted as a function of altitude and longitude every 26 deg for SAM II measurements on Aug. 2-3, 1979, at a latitude of 71-deg N. The continuous vertical line is the zero meridian. The contours are scaled by 10^{-5} km^{-1} and are separated by a factor of 1.32. Again, the typical background value of 1.2×10^{-4} km^{-1} is shown at all longitudes for the aerosol layer in the lower stratosphere. Tropospheric clouds are shown below the local tropopauses (marked with crosses inside circles) and represent very high values. The tic marks on the horizontal axis correspond to the longitudes of SAM II measurements used to construct this isopleth.

The occurrence of polar stratospheric clouds (PSC's) in the Antarctic wintertime is shown in Fig. 5. Large values of extinction are found throughout most of the lower stratosphere. These high values are coincident with very low temperatures in every case. The role of these PSC's, which are being found throughout the Antarctic winter and to a lesser degree during the Arctic winter, will have to be considered in water vapor and radiation budget studies.[9]

Concluding Remarks

This Note has described the developing global data set for stratospheric aerosols that is evolving from the satellite sensors SAM II and SAGE. It has presented typical values and the enhanced values after the violent eruption of Mount St. Helens which increased the Northern Hemisphere aerosol mass by an order of magnitude. The existence of polar stratospheric clouds has also been described. These are seen to occur in the polar winters associated with very cold atmospheric air masses and to increase extinction by an order of magnitude and more.

Acknowledgments

The author wishes to thank the SAM II and SAGE science teams and members of the Langley Research Center SAM II and SAGE engineering and experiment teams that made these data possible.

References

[1] Junge, C. E., Chagnan, C. W., and Manson, J. E., "Stratospheric Aerosols," *Journal of Meteorology*, Vol. 18, Feb. 1961, pp. 81-108.

[2] Hofmann, D. J. and Rosen, J. M., "On the Background Stratospheric Aerosol Layer," *Journal of the Atmospheric Sciences*, Vol. 38, Jan. 1981, pp. 168-181.

[3] Russell, P. B., Swissler, T. J., McCormick, M. P., Chu, W. P., Livingston, J. M., and Pepin, T. J., "Satellite and Correlative Measurements of the Stratospheric Aerosol. I: An Optical Model for Data Conversion," *Journal of the Atmospheric Sciences*, Vol. 38, June 1981, pp. 1279-1294.

[4] Rosen, J. M., "The Boiling Point of Stratospheric Aerosols," *Journal of Applied Meteorology*, Vol. 10, Oct. 1971, pp. 1044-1046.

[5] Toon, O. B. and Pollack, J. B., "Atmospheric Aerosols and Climate," *American Scientist*, Vol. 68, May-June 1980, pp. 268-278.

[6] McCormick, M. P., Hamill, P., Pepin, T. J., Chu, W. P., Swissler, T. J., and McMaster, L. R., "Satellite Studies of the Stratospheric Aerosol," *Bulletin of the American Meteorological Society*, Vol. 60, Sept. 1979, pp. 1038-1046.

[7] Chu, W. P. and McCormick, M. P., "Inversion of Stratospheric Aerosol and Gaseous Constituents from Spacecraft Solar Extinction Data in the 0.38-1.0 μm Wavelength Region," *Applied Optics*, Vol. 18, May 1979, pp. 1404-1413.

[8] Hansen, J. E., Wang, W. C., and Lacis, A. A., "Mount Agung Eruption Provides Test of a Global Climatic Perturbation," *Science*, Vol. 199, March 1978, pp. 1065-1067.

[9] McCormick, M. P., Steele, H. M., Hamill, P., Chu, W. P., and Swissler, T. J., "Polar Stratospheric Cloud Sightings by SAM II," *Journal of the Atmospheric Sicences*, Vol. 39, June 1982, pp. 1387-1397.